# Prediction of Power Chimney Parameters Influenced the Operation at Nassiriya City

**Rafid M. Hannun**
Elect. Eng. Dept.
College of Engineering
Thi-Qar University

**Adnan A.A.**
Mech. Eng. Dept.
College of Engineering
Thi-Qar University

**Ghassan Adnan Abd**
Mech. Eng. Dept.
College of Engineering
Thi-Qar University

## Abstract

The power chimney tower is one of modern promised energy which may be developed by low losses, simple and has high facilities.

In this paper, many parameters were studied for prediction of system operation. Velocity distribution is the important parameter which gives the first prediction to put the position of erection of power turbine, made or not. The numerical analysis was presented by using GAMBIT and FLUENT 6.3 to predict that high velocity at the expansion of chimney near the solar collector place. This position is very suitable for promoting and building the power turbine since the velocity range was between (33 - 54 m/s) for different solar flux 200W/$m^2$, 400W/$m^2$, 600W/$m^2$ and 800W/$m^2$. So, the other factors, temperature and pressure were studied to coincide with previous papers in this field.

## المستخلص

إن مدخنة القدرة واحدة من أهم الأساليب الحديثة في توليد الطاقة لسهولتها وقلة مفاقيدها وتعقيداتها.
في هذا البحث, تمت دراسة عدة عوامل لها تأثيراً على عمل المنظومة. واهم هذه العوامل هو توزيع السرعة الذي ينبئ أولاً بموقع تنصيب تربين القدرة, يوضع في هذا أو في غيره. تم تقديم تحليل عددي وباستخدام برنامج الكامبتوالفلونت للتنبؤ بمكان أعلى سرعة قرب توسع المدخنة في مركز قاعدة غطاء المجمع الشمسي. حيث إن هذا المكان هو الأكثر ملائمة لبناء تربين القدرة ودعمه لكون سرع الهواء قد وصلت إلى مديات تتراوح بين (33 و 54 م/ثا) عند تسليط إشعاع شمسي بمعدل (200, 400, 600, 800) واط/$م^2$ . كذلك تمت دراسة العوامل الأخرى المؤثرة على كفاءة المنظومة مثل درجة الحرارة وفرق الضغط وتبين إنها متوافقة لما تم دراسته سابقا من قبل الباحثين في أدبيات الموضوع.

## 1- Introduction

Solar energy is an abundant renewable and clean source free of green house gases emissions. Solar power plant is very important use of this energy. Solar chimney technology is a promising large scale of power generation. This technology was first described by Gὒnter in 1931 and tested with the 50 kw Manzanares prototype plant since 1980. There are three components for the combination of this prototype: solar collector, turbine connected with electrical generator.

The installation of solar chimney power plant at Nassiriya city (31.036˚N, 46.21˚E) is suitable to get high energy generated as a result to high rate of solar flux incident as high as flux in the world regions [1].

The incident solar flux on the inclined circular frame of glass layers passes through to black ground at the floor. The air near the ground absorbs the heat to decrease its density. The hot air particles move up to hit the glass ceiling continuously and go to chimney vent. This series heating generates continuous movement of air, then, generates electrical energy by installing turbine connected to electrical generator. The height of chimney causes high pressure difference between the upper and lower points. This pushes increasingly the movement of air particles between the lower points of chimney to up.

Main features of a solar chimney power plant area circular green house type collector and a tall chimney and its centre. Air flowing radial inwards under the collector roof heats up and enters the chimney after passing through a turbo generator [2].

Backstrom and Fluri [2] developed two analyses for finding the optimal ratio of turbine pressure drop to available pressure drop in a solar chimney power plant to be 2/3 for maximum fluid power and using the power law model for this prediction. Haaf et al. [3] , Haaf [4] and Schlaich [5] described the operation and presented results for a prototype solar chimney power plant built in Manzanares, Spain in 1982.

Pretorius and Kröger [6] evaluated the influence of a recently developed convective heat transfer equation, more accurate turbine inlet loss coefficient, quality collector roof glass and various types of soil on the performance of a large scale solar chimney power plant. This simulation of study concluded that the new heat transfer equation reduce the annual plant power output by 11.7%, but , the more realistic turbine inlet loss coefficient only accounts for a 0.66˚rise in annual power production , while utilizing better quality glass increases the annual plant power output by 3.4%.

Tingzhen et. al. [7] carried out numerical simulations on the solar chimney power plant system which divided into three regions: the collector, the chimney and the turbine, and the mathematical models of heat transfer and flow had been setup for these regions. Ming et. al. [8] performed to analyze the characteristics of heat transfer and air flow in the solar chimney power plant system with an energy storage layer. They used different mathematical models for the collector, chimney and the energy storage and the effect of solar radiation on the heat storage characteristic of the energy storage layer. Nizetic et. al. [9] analyzed the feasibility of solar chimney power plants for small settlements and islands of countries in the Mediterranean region; they used 550 m height of chimney with collector roof diameter of 1250 m to produce 2.8 – 6.2 MW of power.

Ninic and Nizetic [10] developed and use of the availability of warm, humid air via the formation of up draft "gravitational vortex column" situated over turbine with numerical solution for solar chimney power plant. Petela [11] used a simplified model of solar chimney power plant which consists of a heating air collector, turbine and chimney to interpretate a thermodynamic based on the derived energy and energy balances. Zhou et. al. [12] analyzed the suitable chimney height of solar chimney power plant using a thermodynamic model validated with the measurements of the only one prototype in Manzanares.

## 2- Numerical model

### 2-1 Physical model

In this study, some practical prototype from literature depended on as shown in Figure 1 is selected as a physical model for simulation. The chimney height is 100 m and radius 2.5 m, the collector of 120 m radius and 2m height Figure1.

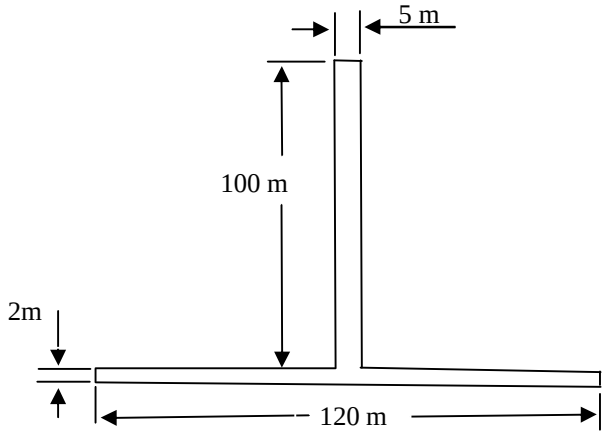


**Figure (1). Physical prototype.**

**2-2 Mathematical model**

There are many prototypes in the world have large different heights up to 500 m , with different radii of chimney but with low heights for collector (up to 3m) with wide radii. The model of 100m height of chimney and 2.5 m its radius and the collector of 60m radius and 2 m height are used. The storage layer of energy such as soil or graved coated by asphalt is the solid matrix of this collector.

The buoyancy induced as natural convection is measured by Rayleigh number (Ra):

$R_a = g\beta(T_h-T_C)L^3/a\upsilon$

Where $T_h$,$T_C$ is the maximum and minimum temperature of the system respectively. The Ra in this system analysis shows that Ra> 10^10, therefore the flow is turbulent. The continuity, Navier – Stokes, energy equations and k-ε equation are shown below[9]:

$$\frac{\partial r}{\partial t}+\frac{\partial(ru)}{\partial x}+\frac{\partial(ry)}{\partial y}=0 \tag{1}$$

$$\frac{\partial(ru)}{\partial t}+\frac{\partial(ruu)}{\partial x}+\frac{\partial(rvu)}{\partial y}=rgb(T-T_\infty)+m\left(\frac{\partial^2 u}{\partial x^2}+\frac{\partial^2 u}{\partial y^2}\right) \tag{2}$$

$$\frac{\partial(rv)}{\partial t}+\frac{\partial(ruv)}{\partial x}+\frac{\partial(rvv)}{\partial y}=-\frac{\partial p}{\partial y}+m\left(\frac{\partial^2 v}{\partial x^2}+\frac{\partial^2 v}{\partial y^2}\right) \tag{3}$$

$$\frac{\partial(rcT)}{\partial t}+\frac{\partial(rcuT)}{\partial x}+\frac{\partial(rcvT)}{\partial y}=l\left(\frac{\partial^2 T}{\partial x^2}+\frac{\partial^2 T}{\partial y^2}\right) \tag{4}$$

$$\frac{\partial}{\partial t}(rK)+\frac{\partial}{\partial x_i}(rKu_i)=\frac{\partial}{\partial x_j}\left(\left(m+\frac{m_t}{s_K}\right)\frac{\partial K}{\partial x_j}\right)+G_K+G_b-re+S_K \tag{5}$$

$$\frac{\partial}{\partial t}(re)+\frac{\partial}{\partial x_j}(reu_i)=\frac{\partial}{\partial x_j}\left(\left(m+\frac{m_t}{s_K}\right)\frac{\partial e}{\partial x_j}\right)+C_{ie}(G_K+C_{3e}G_b)-C_{2e}r\frac{e^2}{K}+S_e \tag{6}$$

The heat transfer in the energy storage layer may be very complicated [8]. The Brinkman – Forchheimer Extended Darcy model may be used in this paper for storage material as regarded as porous media, as follows:

$$\frac{\partial r}{\partial t}+\frac{\partial(ru_d)}{\partial x}+\frac{\partial(rv_d)}{\partial y}=0 \tag{7}$$

$$\frac{r}{j}\frac{\partial u_j}{\partial t}+\frac{r}{j^2}\left(u_d\frac{\partial u_j}{\partial x}+v_d\frac{\partial u_d}{\partial y}\right)=-\frac{\partial P_r}{\partial x}+\frac{\partial}{\partial x}\left(m_m\frac{\partial u_d}{\partial x}\right)+\frac{\partial}{\partial y}\left(m_m\frac{\partial u_d}{\partial y}\right)-\left(\frac{m}{K}+\frac{rc}{\sqrt{K}}u_d\right)u_d+rgb(T-T_\infty) \tag{8}$$

$$\frac{r}{j}\frac{\partial v_j}{\partial t}+\frac{r}{j^2}\left(u_d\frac{\partial v_j}{\partial x}+v_d\frac{\partial v_d}{\partial y}\right)=-\frac{\partial P_r}{\partial x}+\frac{\partial}{\partial x}\left(m_m\frac{\partial v_d}{\partial x}\right)+\frac{\partial}{\partial y}\left(m_m\frac{\partial v_d}{\partial y}\right)-\left(\frac{m}{K}+\frac{rc}{\sqrt{K}}v_d\right)v_d \quad (9)$$

$$rc\left(\frac{\partial T}{\partial t}+u_d\frac{\partial T}{\partial x}+v_d\frac{\partial T}{\partial y}\right)=\frac{\partial}{\partial x}\left(l_m\frac{\partial T}{\partial x}\right)+\frac{\partial}{\partial x}\left(l_m\frac{\partial T}{\partial y}\right) \quad (10)$$

The heat balance of the storage layer is Shown in Figure(2) with the related equations:

$$Q1+Q2+Q3+\zeta\tau Q4 = 0 \quad (11)$$

Where ……..

$$Q_1=A_1h_1(T_1 - T_2) \quad (12)$$

$$Q_2 = A_2\,б\,(T_1^4 - T_2^4) \quad (13)$$

$$Q_3 = -A_1\,\lambda_m dT/dx \quad (14)$$

The heat balance of the collector glass:

$$Q_5 + Q_6 – Q_2 +Q_7 +\alpha Q_4 = 0 \quad (15)$$

Where :

$$Q_5= A_2h_2(T_g-T_a) \quad (16)$$

$$Q_6 = A_2h_3\,(T_g-T_4) \quad (17)$$

$$Q_7 = A_2\,б\,(T_g^4 – T_5^4) \quad (18)$$

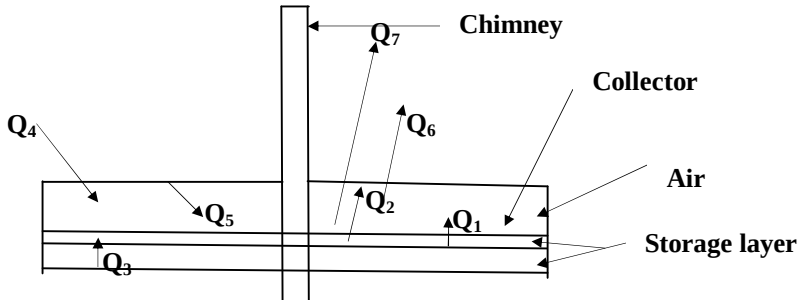


**Figure (2).Heat balance of the storage layer and the collector glass.**

## 2-3 Boundary conditions

1. **For chimney**

$$\frac{\partial T}{\partial X} = 0\,, u = 0\,, v = 0 \quad (19)$$

For outside and inside the storage layer

$$\frac{\partial T}{\partial y} = 0\,, u_d = 0, v_d = 0 \quad (20)$$

For outlet conditions:

At x= ± ∞, T = $T_4$, P = $P_{atmosphere}$ (21)

**2. Symmetrical axis at chimney centre axis, i.e:**

$$u_{(x=+x)} = u_{(x=-x)}\ , v_{(x=+x)} = v_{(x=-x)}, p_{(x=+x)} = p_{(x=-x)} \quad (22)$$

$$m_m\left(\frac{\partial u_d}{\partial y}+\frac{\partial v_d}{\partial x}\right)_{(x=+x)} = m_m\left(\frac{\partial u_d}{\partial y}+\frac{\partial v_d}{\partial x}\right)_{(x=-x)} \quad (23)$$

## 3- Numerical analysis

The turbulent flow of air inside the system would be analyzed by standard k-ε model, and the energy storage layer can be described by using Brinkman- Forcheimer Extended Darcy model. The SIMPLE algorithm with QUICK Scheme method used to solve the pressure – velocity coupling and momentum and energy equations respectively. These methods were explained by many references such as Ref.[13]. So, the Gambit and Fluent Codes are used to describe the results of this paper Figure3 the study case of chimney system as designed by GAMBIT).

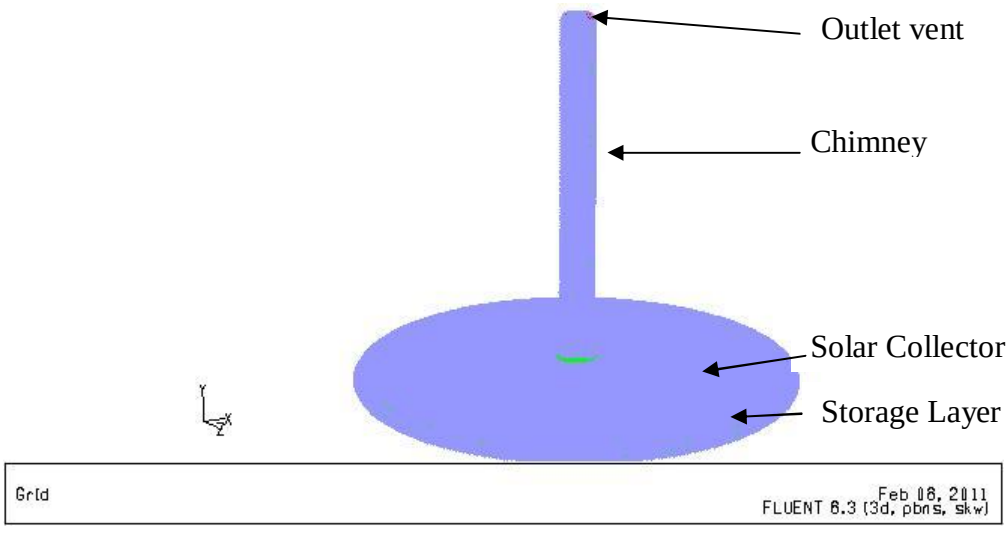


**Figure(3) . The domain grid as designed by GAMBIT code on Feb. 8, 2011 .**

## 4- Results and discussion

The heat energy transferred from the solar rays by beam or diffused arrays to glass cover of collector. Then, they transferred to the storage layer depending on high permeability and transmittance, with low reflectance and absorbance of glass cover. In addition to high absorbance low high reflection of storage layer with ability of high convective heat transfer rate.

Many materials and mixtures arranged for storage layers depend on the enhancement of heat transferred from this layer to air inside the collector of solar chimney. Low storage ratio for a lot of materials lies at 600 $W/m^2$ of solar radiation as mentioned by many researchers [13].

In this paper, four cases of solar radiation fluxes are studied for Al- Nassiriya city case study which lies at 31.036° N, 46.21° E. The cases are 200, 400, 600, 800 $W/m^2$ of solar flux.

There are many reasons for the selection of turbine erection position inside the chimney requires further discussion. The first factor is the difference in static pressure gradient as shown in Figure ( 4 and 5).

At a 200 $W/m^2$ solar flux absorbed by storage layer and transferred as heat to neighbor air inside collector by convective heat transfer shape. The figure arranged by Cartesian coordinates X-Y-Z as shown. High differences in static pressure values(- $1.27x10^{+3}$ to $3.8x10^{-1}$) are measured between the upper point of chimney as low pressure value to high value at the base outer circumference of collector. This high difference is created because of high height of chimney and the heat absorbed by air which accelerates the air velocity cause high relative pressure. It is observed that there are high difference between the gradient of chimney and collector. Therefore, this is one of reasons for turbine installation at this base. Furthermore, from the other shapes of Figure(4 B, C, D), it is seen that the relative static pressure changed significantly with increasing the solar radiation (from 400 $W/m^2$ to 800 $W/m^2$) . That is because of increasing the air density inside the collector in comparison with environment of station at the same altitude. This heat transferred with natural convection to increase the pressure gradient which reach the levels between ($-1.3 \times 10^{-3}$ Pa to $3.95 \times 10^{-1}$Pa), ($-1.83 \times 10^{+3}$Pa to 5.72Pa) and ($-1.67 \times 10^{+3}$ Pa to $6.68 \times 10^{+2Pa}$) for 400, 600 and 800 $W/m^2$ of solar radiation intensity.

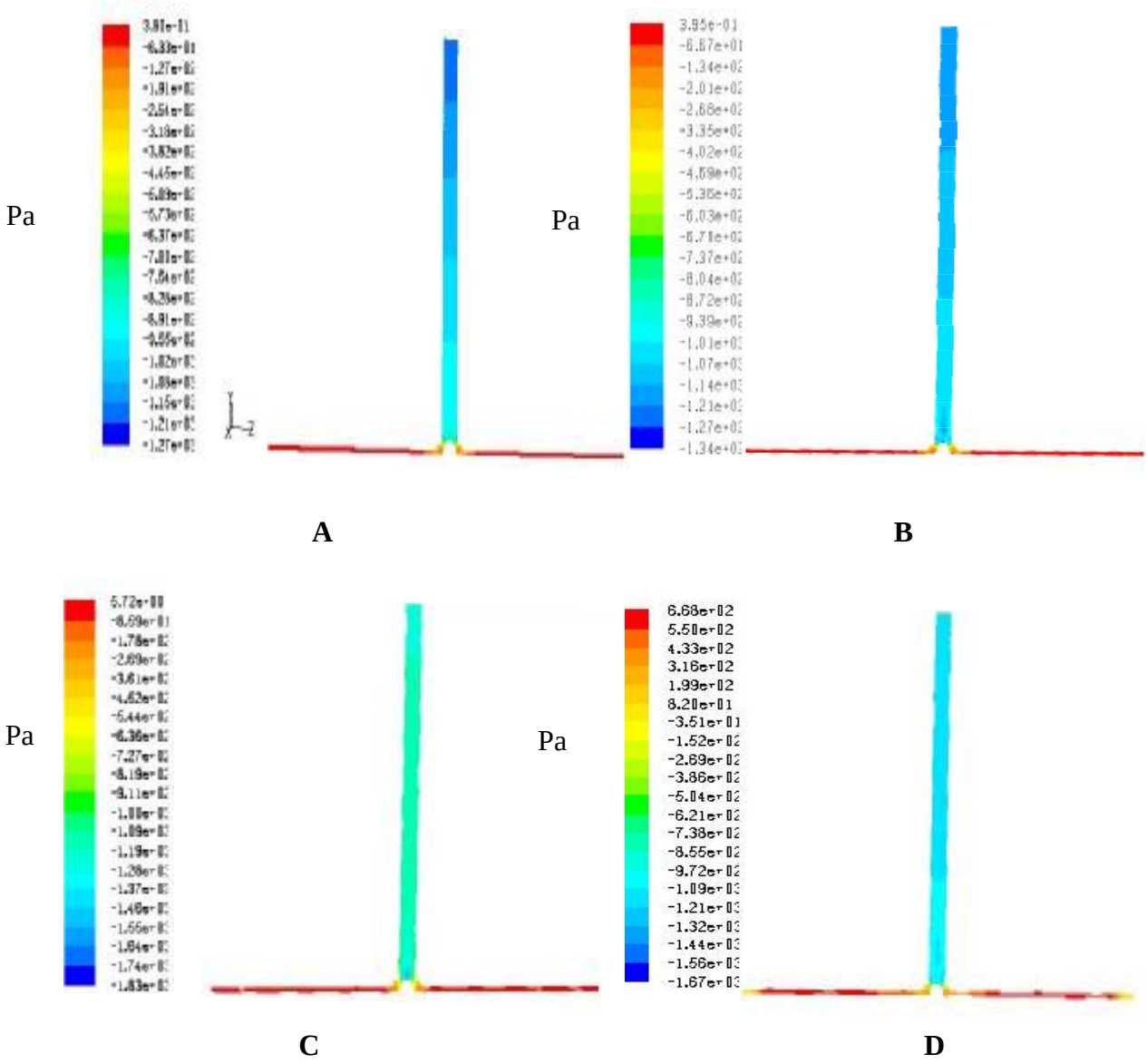


**Figure(4). Pressure gradient at A. 200W/m$^2$, B. 400W/m$^2$, C. 600W/m$^2$ and D. 800W/m$^2$ of solar flux.**

Figure(5) shows the static pressure distributions which is calculated from the central section of whole domain as circumferential mean values which be sure the validity of this study and prove the mentioned pressure values. The maximum values of pressure are for 800W/m$^2$ solar flux, but the minimal values are for 200W/m$^2$. So, the other values of solar flux lie between the previous lines. The pressure gradient is approached to atmosphere at the inlet vent of the system but it is increased while reach the top of chimney since high difference in relative pressure due to the heat and height of chimney which work as vacuum pressure to increase the air velocity.

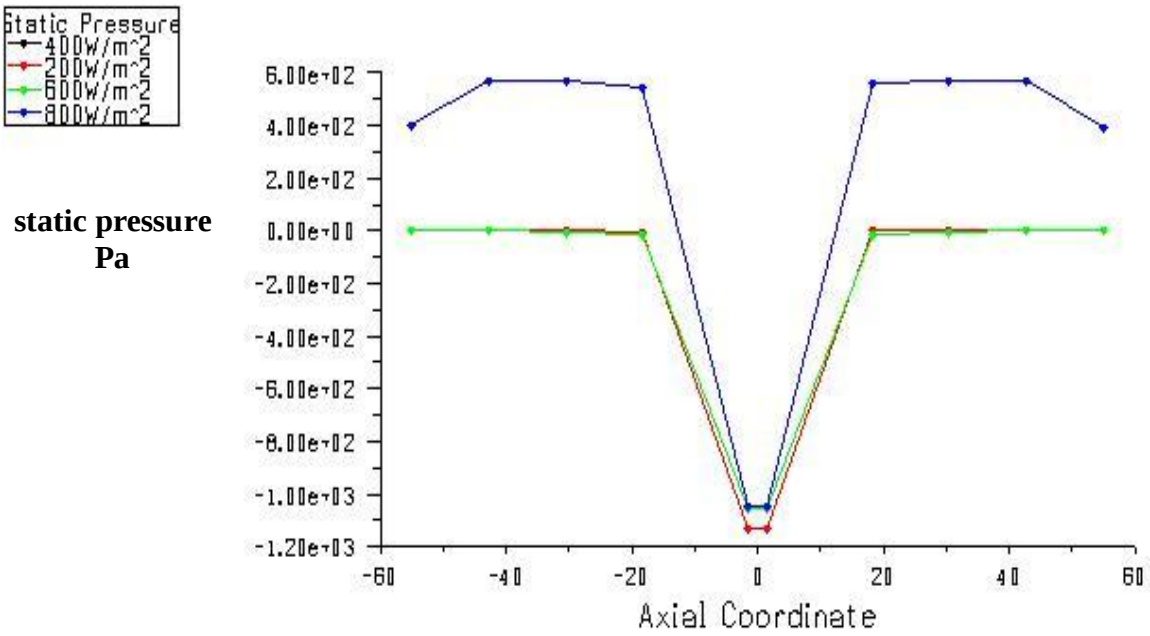


**Figure(5). Static pressure of domain calculated for central section plane.**

Figure(6) shows the temperature distribution inside the system of solar chimney. Figure (5 A) is an indication of heat absorbed or transferred to different trends of parts chose at 200 W/m$^2$ of solar radiation intensity. This shape of temperature range (534 K to 299 K) which is at ambient temperature of 308 K.

FLUENT Code demonstrates wide ranges of measurements near the effective domain. The dominated temperature of air inside the chimney is 319K as observed by limited range contour which shown in Figure(6B). The Figure6C denotes to the high temperature recorded at the end edge of circular collector at the base which is corresponded to solar storage layer. It is notably high hot place than collector space because the heat coefficient at the end has low value as a result to low velocity of convicted air. This air speed increases in the direction of chimney centre.

The other shapes of Figure(6 D, E and F )denote to temperature difference at solar flux of 400, 600 and 800W/m$^2$ respectively. It is normally, there are gradually higher temperature ranges than 200W/m$^2$ of solar flux mode. This heat forces the velocity magnitude in the direction of chimney centre as a result to natural convection.

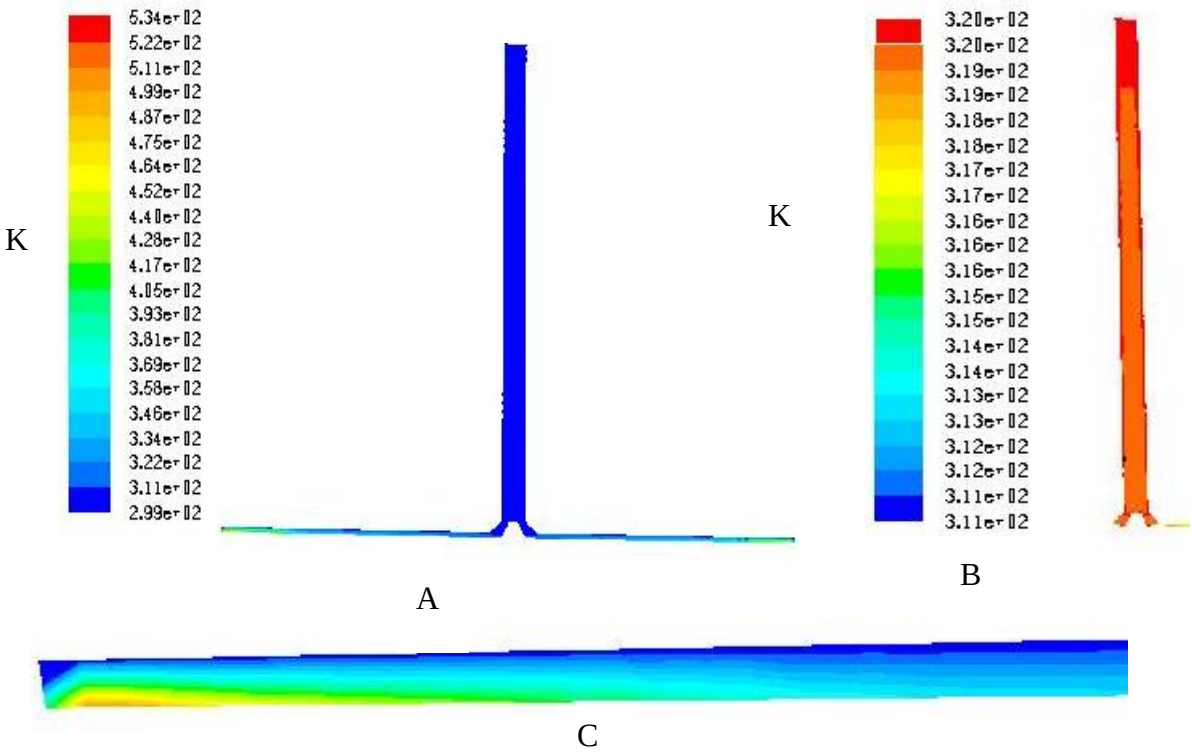


**Figure(6). Static temperature at 200W/m$^2$ solar flux for A. the system, B. chimney and C. collector section.**

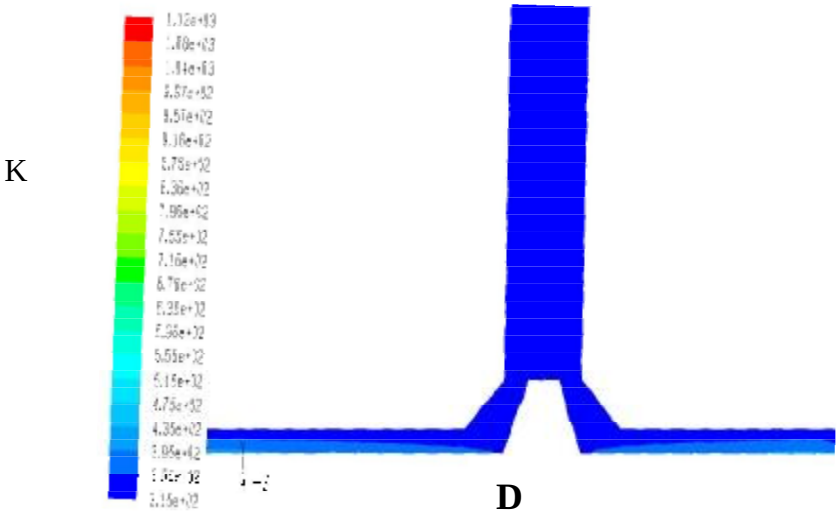


**Figure (6). Static temperature at D. 400W/m$^2$.**

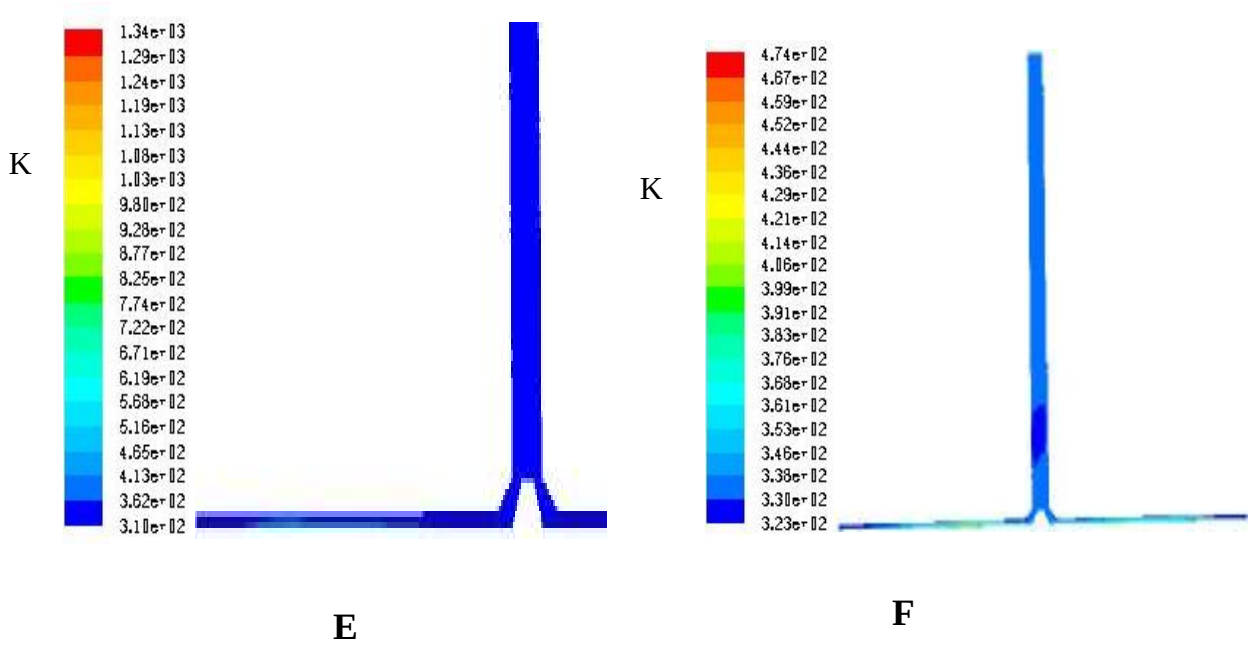


**Figure( 6). Static temperature at E.600W/m$^2$, and 800W/m$^2$ solar flux.**

Figure(7) shows the circumferential average static temperature values for 200W/m$^2$ solar flux radiation and the upper value of it (800W/m$^2$). This indicated dramatically the previous conclusion that the high flux has high temperature values reverse to lower flux which has low temperature gradient. So, there are some points take different slop from the other points of the curve as a result to turbulent flow of flowing air in this section and all other sections. The maximum values of temperature trend from the free edges in the direction of chimney centre since the continuous solar heating from the outer edge to inner collector parts. This is in agreement with literature.

The velocity vectors of the system are shown in Figure(8) which indicates that high velocity magnitude at concentration of solar radiation flux 200W/m$^2$ reaches 33m/s at the position of turbine at the lower part of chimney with no load state as shown in A. So, there is a low velocity gradient at the outer end of collector of the base part of system. The velocity notably increases when directed to the chimney centre due to the heat flux increase, narrow area of collector disc and low pressure gradient. The velocity range increases directly with increasing the heat flux of solar array as noted in Figure 8B, C and D. for solar flux 400, 600 and 800W/m$^2$ respectively.

The velocity ranges reach 39, 42, and 54m/s respectively. These ranges are suitable for using big turbines at lower position of chimney or using multi-stage turbine to have high gain energy.

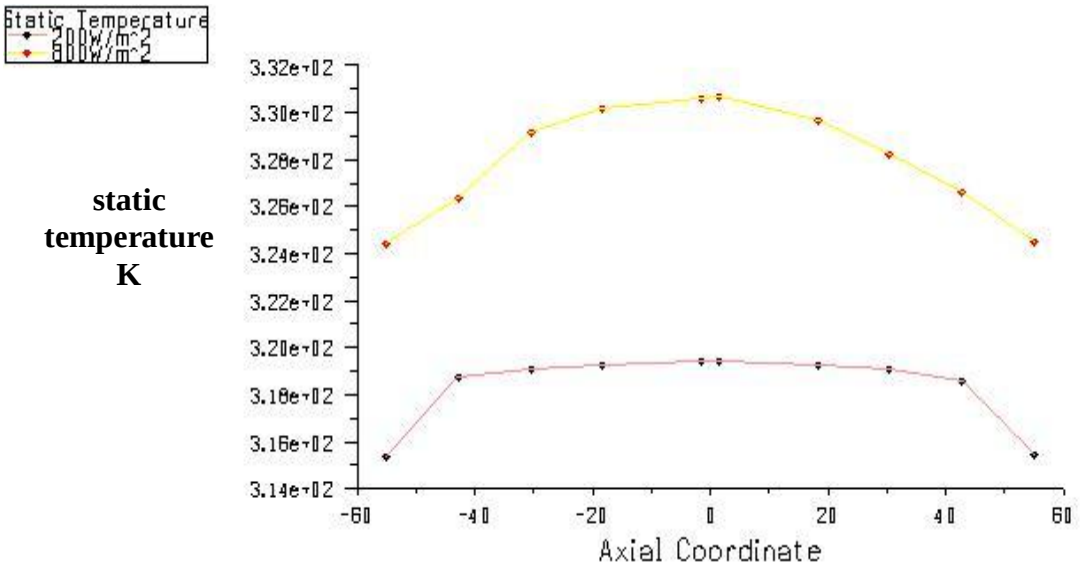


**Figure (7). Circumferential average values of static temperature for lower and upper flux.**

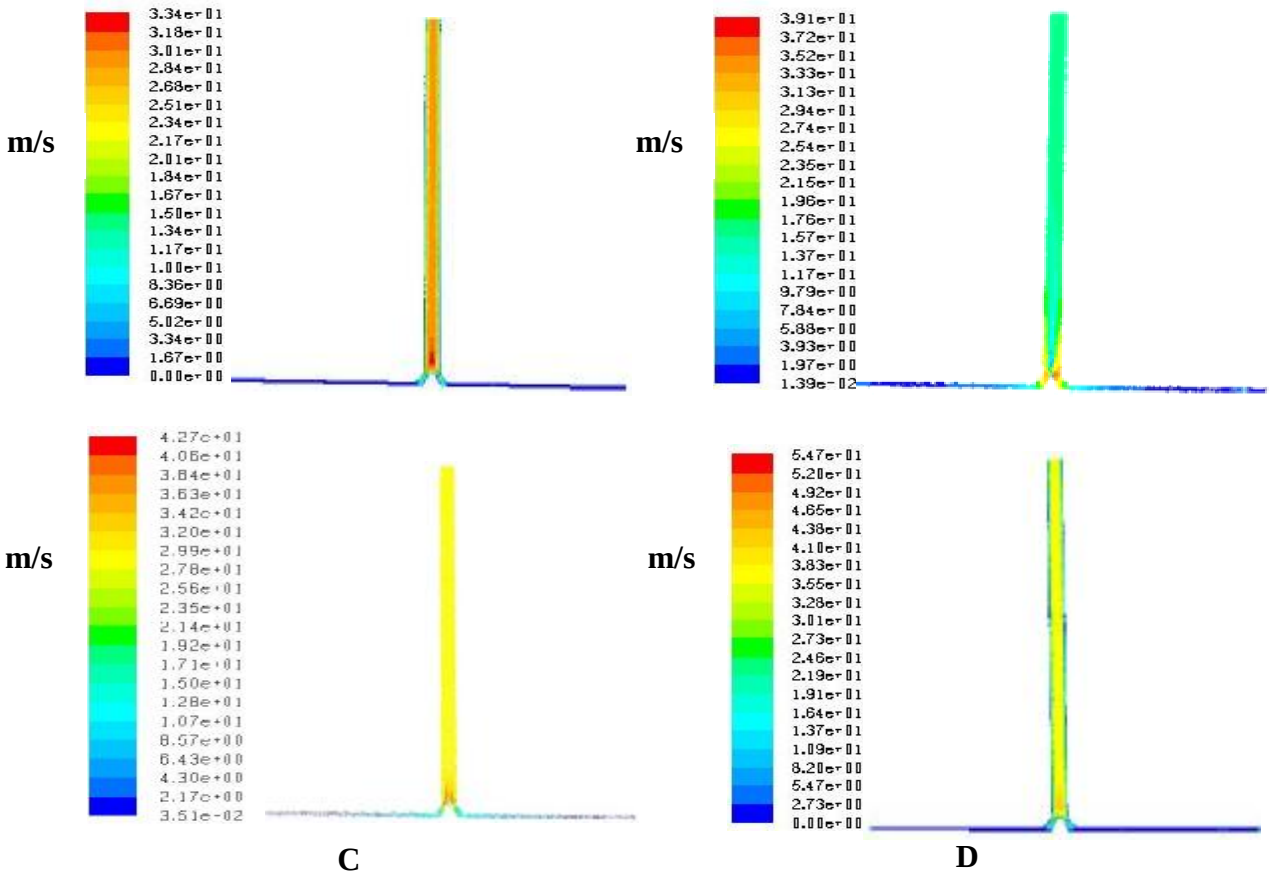


**Figure (8). Velocity distribution at A. 200W/m$^2$, B. 400W/m$^2$, C. 600W/m$^2$ and D. 800W/m$^2$ of solar flux.**

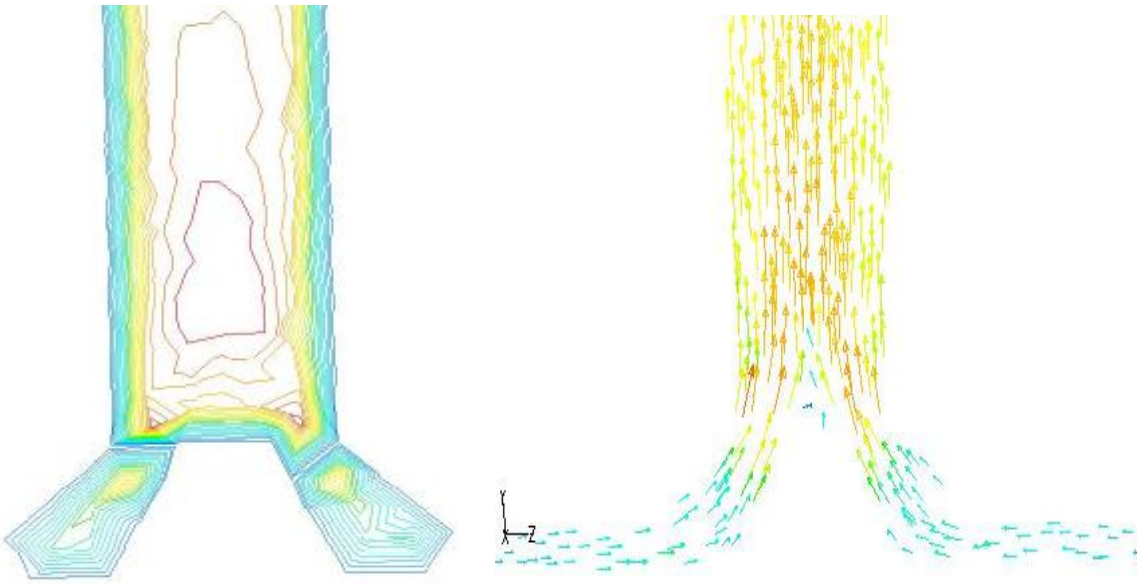

A B

**Figure(9). A-Velocity contours and B-Velocity vectors at the turbine position.**

The velocity stream line of system is shown in Figure(9 A) which denotes high velocity range at the bottom chimney part in the direction of centre. Also, Figure(9 B ) presents the velocity vectors coloured by velocity magnitude which indicates the velocity gradient at the space of system.

The velocity magnitude distribution on the system domain with its position in the centre section for whole system is presented by Figure(10). It is denoted that high velocity values lie at the chimney but low values at the end edges of collector since the reasons mentioned in this paper before.

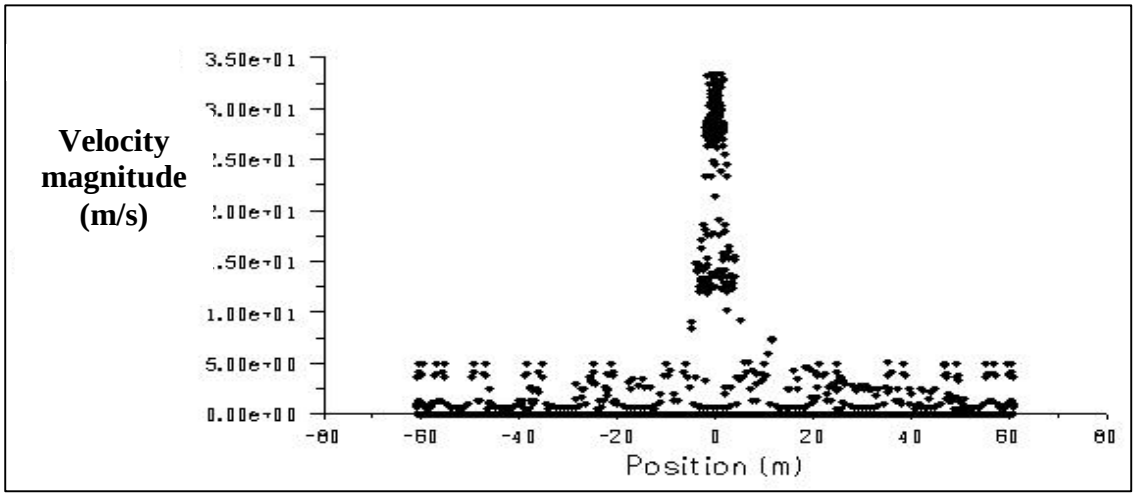


**Figure (10). Velocity magnitude points with position of section centre.**

The upper yellow curve of Figure(11) denotes the velocity magnitudes in the axial coordinate calculated as average values of the central section of domain. It is observed that higher velocity values trend from the outer edge to the central part of domain (chimney) as mentioned before. The other curves give the same conclusion, but there are some values for collector edge put as higher than the inner because of turbulent flow with axial values at this section which may be made lower at neighbor section.

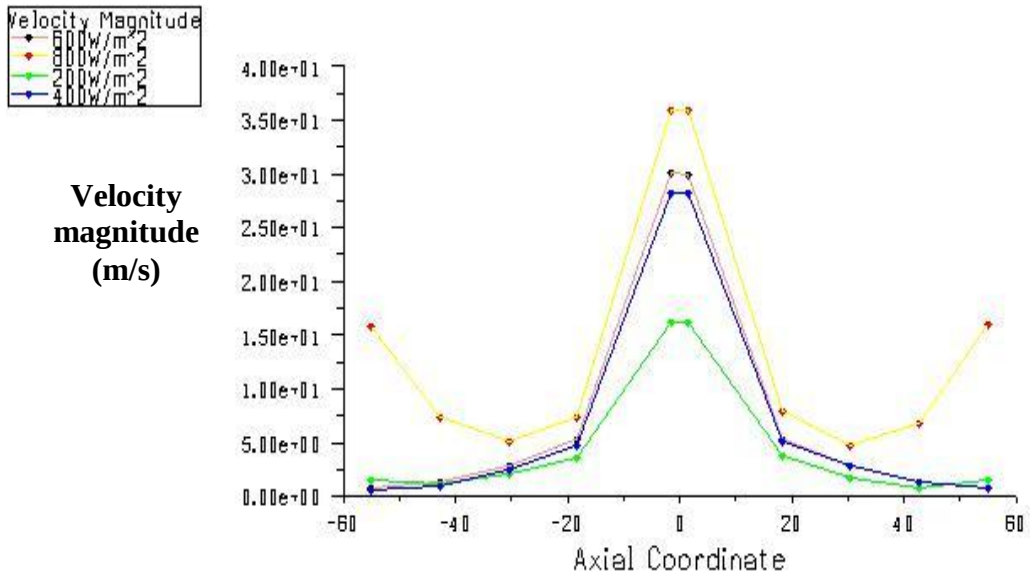


**Figure(11). Circumferential average of velocity magnitude for different solar flux.**

## 5- Conclusions

It is noted from the numerical solution and the analysis of chimney tower system for the predicted case study for Nassiriya city, there are some conclusions presented about the circumferential parameters such as:

1. The velocity of air is high at the base section of chimney but it is very low at the outer edge of collector canopy and then converged in developing to the chimney centre.
2. The temperature of storage wall of solar heat flux is highest as a result to heat absorption but it is low in the chimney due to air movement with heat transferred inside the system.
3. The pressure gradient is approached to atmosphere at the inlet vent of the system but it is increased while reach the top of chimney since high difference in relative pressure due to the heat and height of chimney which work as vacuum pressure to increase the air velocity.
4. Due to the high velocity recorded at the expansion of chimney, the turbine power is preferred to built-in.

## 6- References


[1] Hannun R.M.,2005, " Modeling of Solar Thermal Power Plant" , M.Sc. thesis, University of Technology, Mechanical Engineering Department, Baghdad.

[2] Backström T. and Fluri T. , 2006," Maximum Fluid Power Condition in Solar Chimney Power Plants –An Analytical Approach", Solar Energy 80, pp. 1417-1423.

[3] Haaf W., Friedrich K., Mayr G., Schlaich J.,1983, "Solar Chimneys, Part I: Principle and Construction of the Pilot Plant in Manzanares", International Journal of Solar Energy 2, 3–20.

[4] Haaf W., 1984,"Solar Chimneys, Part II: Preliminary Test Results From the Manzanares Pilot Plant", International Journal of Solar Energy 2, 141–161.

[5] Schlaich J., 1994,"The Solar Chimney: Electricity from the Sun", Deutsche Verlags-Anstalt, Stuttgart.

[6] Pretorius J. P. and Kröger D.G. ,2006,"Critical Evaluation of Solar Chimney Power Plant Performance ", Solar Energy 80, pp. 535 -544.

[7] Tingzhen M., Weil., Guoling X., Yanbin X., Xuhu G. and Yuan P., 2008,"Numerical Simulation of the Solar Chimney Power Plant Systems Coupled with Turbine", Renewable energy 33, pp. 897-905.

[8] Ming T., Liu W. , Pan Y. and Xu G., 2008," Numerical Analysis of Flow and Heat Transfer Characteristics in Solar Chimney Power Plant with Energy Storage Layer", Energy Conversion and Management 49,pp. 2872-2879.

[9] Nizetic S. , Ninic N. and Kalrin B., 2008," Analysis and Feasibility of Implementing Solar Chimney Power Plants in the Mediterranean Region", Science direct, Solar Energy 33, pp. 1680-1690.

[10] Ninic N. , Nizetic S., 2009,"Elementary Theory of Stationary Vortex Columns for Solar Chimney Power Plants", Science direct, Solar Energy 83, pp476-476.

[11] Petela R. , 2009,"Thermodynamic Study Of A Simplified Model of the Solar Chimney Power Plant ", Science direct, Solar Energy 83, pp. 94-107.

[12] Zhou X., Yong J., Xiao B. Hou G., and Xing F., 2009,"Analysis of Chimney Height for Solar Chimney Power Plant" Applied Thermal Engineering 29, pp.178-185.

[13] Tao WQ., 2001,"Numerical Heat Transfer", 2nd ed. Xi'an, China: Xi'an Jiaotong University Press.


## 7- Nomenclature

| Symbol | Definition |
|---|---|
| A | Thermal diffusivity ( $m^2/s$). |
| $A_1$ | The area of storage layer surface( $m^2$). |
| $A_2$ | Glass area ( $m^{2)}$ |

| | |
|---|---|
| G | Gravitational body force ($m/s^2$) |
| $H_1$ | The heat transfer coefficient between the storage layer and the air inside the collector( $W/m^2K$). |
| $h_2$ | Convection heat transfer coefficient between the surface of glass and air ($W/m^2K$). |
| $h_3$ | The convective heat transfer coefficient ( $W/m^2K$) |
| L | Collector height ( m) . |
| $Q_1$ | The heat transfer between the storage layer and the air (W). |
| $Q_2$ | The radiation heat transfer between the storage and the collector glass (W). |
| $Q_3$ | The conduction heat transfer from the storage inside the porous media (W). |
| $Q_4$ | The solar heat flux transferred to the collector (W). |
| $Q_5$ | The convective heat transfer between the glass surface and the air inside the collector (W). |
| $Q_6$ | The conduction heat transfer between the collector surface and the ambient (W). |
| $Q_7$ | The radiation heat transfer between the collector surface and the sky (W). |
| $R_a$ | Rayleigh number |
| $T_1$ | The storage layer temperature(K). |
| $T_2$ | The air temperature inside the collector (K) |
| $T_3$ | Glass collector temperature (K). |
| $T_4$ | The ambient temperature (K) |
| $T_a$ | Air temperature inside the collector(K) |
| $T_g$ | Glass temperature (K). |
| $T_s$ | Sky temperature (K). |
| $\beta$ | Coefficient of Thermal expansion (1/K) |
| $\lambda_m$ | The heat conduction coefficient ( W/mK) |
| $\mu$ | Dynamic viscosity (kg/m.s) |
| $\nu$ | Kinematic viscosity ($m^2/s$) |
| $\rho$ | Density ($kg/m^3$) |
| $\tau$ | The transmissivity of the collector glass to the solar radiation. |
| б | Stefan-Boltzman constant( $W/m^2K^4$) |